ACS APPLIED MATERIALS & INTERFACES

Research Article

www.acsami.org

Dry-Spun Single-Filament Fibers Comprising Solely Cellulose Nanofibers from Bioresidue

Saleh Hooshmand,[†] Yvonne Aitomäki,[†] Nicholas Norberg,[§] Aji P. Mathew,[†] and Kristiina Oksman*[,†]

[†]Division of Materials Science, Composite Centre Sweden, Luleå University of Technology, Luleå SE-97187, Sweden

[§]PANalytical B.V., Almelo, The Netherlands

ABSTRACT: We demonstrated that low-cost and environmentally friendly filaments of native cellulose can be prepared by dry spinning an aqueous suspension of cellulose nanofibers (CNF). The CNF were extracted from banana rachis, a bioresidue from banana cultivation. The relationship between spinning rate, CNF concentration, and the mechanical properties of the filaments were investigated and the results showed that the modulus of the filaments was increased from 7.8 to 12.6 GPa and the strength increased from 131 to 222 MPa when the lowest concentration and highest speed was used. This improvement is believed to be due to an increased orientation of the CNF in the filament. A minimum concentration of 6.5 wt % was required for continuous filament spinning using the current setup. However, this relatively high concentration is thought to limit the orientation of the CNF in the filament. The process used in this study has a good potential for upscaling providing a continuous filament production with well-controlled speed, but further work is required to increase the orientation and subsequently the mechanical properties.

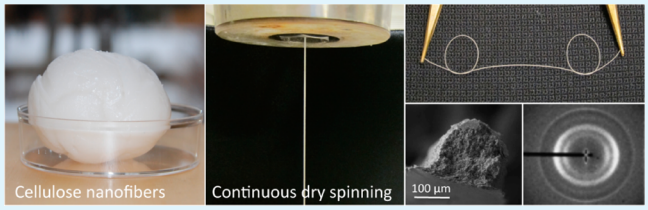

KEYWORDS: *cellulose nanofibers, dry spinning, orientation, filament fibers, mechanical properties, banana rachis*

1. INTRODUCTION

Fibers play an important role for textile and industrial applications in our society. One application for fibers is in polymer composites, where they are combined with polymer matrices to enhance the mechanical properties of the matrix. In structural applications, the highest mechanical properties for composite materials are achieved when fibers are continuous and aligned in the direction of applied load. In recent years, composites made from natural fibers based on cellulose have received increasing attention because they have a low environmental impact and good mechanical properties; for example, soft wood fibers have an approximate modulus of 40 GPa and strength of 1000 MPa.[1,2] The modulus and strength of flax fibers is even higher at 60−80 GPa and 800−1500 MPa, respectively.[3] However, natural fibers are short and discontinuous and the conventional spinning techniques used to produce continuous fibers from them results in yarns with mechanical properties considerably lower than that of the single fiber. For instance, Chabba and co-workers[4,5] reported a Young's modulus between 4.8 and 8.5 GPa and a strength between 312 and 360 MPa for flax yarns. In addition, Goutianos et al.[6] showed that highly twisted yarns led to a degradation of the mechanical properties of the composites, whereas low twisted yarns displayed low processability. Moreover, wide variation and inhomogeneity in the individual fiber properties are considered as another drawback of natural fibers.[5]

One solution in order to overcome the limitations of natural fibers is to prepare continuous biobased fibers and because cellulose is the most abundant biomaterial on the earth, it is an interesting compound from which to prepare manmade fibers. Fibers can be spun from thermoplastic cellulose-based biopolymers such as cellulose acetate (CA) and cellulose acetate butyrate (CAB). However, the low mechanical properties of these polymers make them unsuitable for use in structural composites. Nanoreinforcing of the matrices as well as aligning the polymer chains and nanoreinforcements are two possible ways to increase the modulus and strength of the fibers. Hooshmand and co-workers[7,8] prepared as-spun and drawn melt spun CAB nanocomposite fibers reinforced with cellulose nanocrystals (CNC). Although some improvements were reported due to the nanoreinforcing and partial alignment of the CNC, the final properties of the fibers were still far below the desired values. Indeed a model, which was used to evaluate the reinforcing effect of the CNC, indicated a great potential for aligned CNC to improve the modulus of the fibers.[8]

Regenerated cellulosic fibers (RCF), made by dissolution and precipitation of the cellulose, are another type of continuous cellulosic man-made fiber. RCF are unique in the sense that they have beneficial characteristics of both synthetic and natural fibers, which means on the one hand, they have uniform morphological, mechanical, and physical properties of synthetic fibers, and on the other hand they have biodegradability, CO_2 neutrality, and low density of natural fibers.[9] However, their mechanical properties are lower than that of native cellulose.[10,11] For instance, viscose has a modulus of the 11 GPa and strength of 590 MPa.[2,12] As mentioned earlier,

Received: April 11, 2015
Accepted: May 27, 2015
Published: May 27, 2015

DOI: 10.1021/acsami.5b03091
ACS Appl. Mater. Interfaces 2015, 7, 13022−13028

nanoreinforcing is one way to improve the mechanical properties of the spun fibers. Chen et al.[13] prepared regenerated bacterial cellulose nanocomposite fibers reinforced with multiwalled carbon nanotubes (BC/MWCNT) using N,N-dimethylacetamide/lithium chloride (DMAc/LiCl) as the solvent and ethanol as the coagulation bath. They reported Young's modulus of 29.2 and 38.9 GPa and a strength of ∼600 and ∼500 MPa for regenerated BC fiber and regenerated BC/MWCNT fiber, respectively. Although high mechanical properties of the fibers produced were reported, scaling up of this regenerated BC and use of MWCNT has drawbacks both economically and environmentally.

Of interest is therefore the manufacture of aligned continuous native cellulose fibers. Cellulose nanofibers, which were first successfully isolated in 1983, contain both amorphous and crystalline regions of cellulose.[14,15] CNFs have a high modulus and aspect ratio as well as a large surface area. In addition, the hydroxyl groups on the CNF surface have a strong tendency to bond to each other and form a network.[16] Iwamoto et al.[10] and Walther et al.[17] prepared cellulosic fibers by simply wet spinning tempo-mediated oxidized cellulose nanofibers through a syringe into organic liquids and reported a modulus of ≈23 GPa and strength of ≈400 MPa. Moreover, Torres-Rendon et al.[18] reported a modulus of 33 GPa and strength of 290 MPa for tempo-mediated oxidized cellulose nanofibers spun with the same technique and wet-stretched by ratio of 1.3. Though high mechanical properties of the fibers have been reported,[10,17,18] tempo-mediated oxidation and the solvents used for precipitation do not make the process so economical and environmentally friendly. In another study, Håkansson et al.[19] prepared cellulose filaments by hydrodynamic alignment of carboxymethylated CNF with a flow-focusing channel system to align the fibrils in the flow direction. They used NaCl in the sheath stream and a collecting bath to reduce the electrostatic repulsion of the charged CNF suspension. The fibers were then placed for 24 h in a water bath to allow the electrolytes to diffuse out and finally fixed in acetone and subsequently dried. They reported a modulus of 18 GPa and strength of 445 MPa for the baseline fiber. Although no tempo-oxidation was done, again carboxymethylation and the use of electrolytes and solvent provide some limitations to scaling up and commercializing the process. In a very recent study done by Jiang et al.[20] conductive fibers were produced by wet spinning of only single-walled carbon nanotube (SWCNT) polyelectrolytes and a modulus of 14 GPa and a strength of 124 MPa were reported.

The goal of current study was to, as much as possible, reduce the cost of processing and raw materials in the preparation of aligned cellulosic filaments with high mechanical properties. Thus, a bioresidue from banana rachis was used as the source for the CNFs. This is an ideal source because annually ∼80 MT of bananas are produced in the world, making them the second largest produced fruit with a 16% contribution to the total fruit production.[21,22] This huge amount of production generates a great quantity organic waste. Using this bioresidue will increase the value of the primary product and reduce waste. To the best of our knowledge, this is the first study to show that continuous cellulose fibers can be prepared by dry spinning native cellulose nanofibers without using any chemicals/solvents during the spinning processing. The effect of spinning rates as well as the effect of CNF concentration on the CNF alignment and mechanical properties of the filaments were investigated.

2. EXPERIMENTAL SECTION

2.1. Preparation of Cellulose Nanofibers and Its Dry Spinning. CNFs were isolated from bleached banana rachis pulp, kindly supplied by Pontifical Bolivarian University (UPB), Colombia. The isolation procedure was done using ultrafine grinding with a MKZA10 Super Masscolloider (Masuko Sangyo Co., Saitama, Japan). First, a suspension of 2 wt % was passed through the grinder until a thick gel was formed. The gel was then concentrated to the desired concentrations (8, 10, and 12 wt %) using several steps of centrifugation. Figure 1a shows the concentrated CNF gel with a 10 wt % concentration.

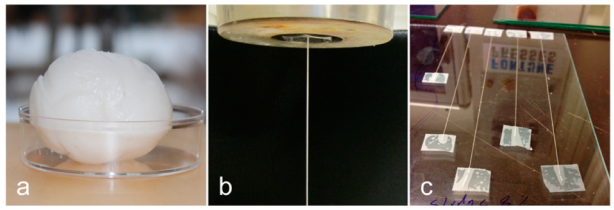

Figure 1. (a) Concentrated CNF (10 wt %), (b) continuous spinning of CNF using the capillary rheometer. and (c) fiber drying process.

All three CNF concentrations (8, 10, and 12 wt %) were dry spun at 25 °C by using a capillary rheometer (Rheo-tester 1000, Göttfert, Buchen, Germany) with 12 mm barrel diameter and 22 cm cylinder length to prepare continuous filaments (Figure 1b). The machine was equipped with a 1 mm single die hole with length of 20 mm and angle of 0°. The CNF was fed manually from top of the rheometer into the capillary and the spinning was carried out using three piston rates (0.5, 1.0, and 1.5 mm/s) and consequently the spinning rates were calculated based on the barrel diameter and die diameter (72, 144, and 216 mm/s). The CNF spun filaments were then collected manually on glass sheets and dried for 10−15 min at room temperature. To avoid shrinkage, we mounted the semidried filaments on the glass sheets using paper tape and kept at room temperature overnight (Figure 1c). Then the dried filaments were placed in the oven at 105 °C for at least for 2 h to remove any remaining moisture. The rheometer used in this study is very similar to piston machines, which are used in the melt spinning of fibers,[23] providing great potential for the process to be scaled up.

To compare the orientation and mechanical properties of the produced filaments with a randomly orientated reference, we prepared a nanofiber network from the same batch of CNF by vacuum filtrating of 100 g of a 1 wt % suspension. The formed cake was then removed from the filter paper and blotted on two dried filter papers. This was repeated three times to remove the excess water. The CNF cake was then placed between two dried filter papers and placed between two woven metal cloths and between two absorbent fabrics. This stack was sandwiched between two metal sheets and dried at 55 °C for 48 h under a load of 450 N. All prepared samples were coded and summarized in Table 1.

2.2. Characterization. *Atomic Force Microscopy (AFM).* To study the morphology of the isolated banana CNF and measure the fibers diameter, a Veeco multimode scanning probe AFM with nanoscope V software (Santa Barbara, CA, USA) was used. The scanning was operated in taping mode and the height image was collected. For the sample preparation, a drop of diluted aqueous CNF suspension was cast on a cleaved mica substrate and dried at room temperature.

X-ray Diffraction (XRD). To determine the crystallinity index of the CNF, we performed XRD using a PANalytical Empyrean (Almelo, The Netherlands) with CuKα radiation with 2θ scan range of 10−40°. The nanopaper made by vacuum filtration was used for this test and the crystallinity index, C_{Ir}, was calculated based on the Segal empirical method[24]

$$C_{Ir}(\%) = \frac{I_{200} - I_{am}}{I_{200}} \times 100 \quad (1)$$

DOI: 10.1021/acsami.5b03091
ACS Appl. Mater. Interfaces 2015, 7, 13022−13028

Table 1. Sample Codes, Wet State Concentration, and Spinning Rate of the Prepared Materials

sample code	CNF concentration (wt %)	spinning rate (mm/s)
CNF-nanopaper	1	
CNF8-72	8	72
CNF8-144	8	144
CNF8-216	8	216
CNF10-72	10	72
CNF10-144	10	144
CNF10-216	10	216
CNF12-72	12	72
CNF12-144	12	144
CNF12-216	12	216

where I_{200} is the peak intensity corresponding to cellulose I, and I_{am} is the peak intensity of the amorphous fraction at $2\theta = 18°$.

Scanning Electron Microscopy (SEM). The fracture cross-section of the filaments broken in the tensile test were studied using a JEOL JSM-6460LV SEM with acceleration voltage of 10 kV. The samples were sputter-coated with gold prior to analysis to avoid charging. In addition, the same instrument was used for filament density measurement based on the weight, length and the average cross section area of several SEM images of different fiber sections using Photoshop CS5.

Extreme High Resolution Scanning Electron Microscopy (XHR-SEM). To study the surface of the spun filaments and possible orientation of the CNFs on the surface of the filaments, a Magellan 400 XHR-SEM (FEI Company, Eindhoven, The Netherlands) was used. The samples were coated with a 3 nm thick layer of platinum before the observation.

Two-Dimensional Wide-Angle X-ray Diffraction (2D-WAXRD). To study the orientation of the CNFs along the filament axis, we performed 2D-WAXRD patterns on spun filaments and the nanopaper using a PANalytical Empyrean multipurpose diffractometer (Almelo, The Netherlands) using Cu-radiation with a wavelength of 0.1540598 nm. The system was equipped with a 2D focusing mirror of Kirkpatrick-Baez type for Cu-radiation focusing on the detector position and a PIXcel^{3D} 2 × 2 detector, imaging a 2θ-range of $\pm 30°2\theta$ with a static exposure. This detector has a pixel size of 55 μm and a detection efficiency of >95% for Cu-radiation. The measurements were performed on single filaments with a measurement time of 15 min per filament. Subsequent data treatment and azimuthal integrations along the diffraction rings were performed using the software packages XRD2DScan and Fit2D.

The orientation index (f_c) was calculated based on azimuthal intensity distribution graphs for the lattice plane of 200 (the most intense peak) according to the following equation[25]

$$f_c = \frac{(180° - \beta_c)}{180°} \quad (2)$$

where the β_c is the full width at half-maximum of the azimuthal peak.

Tensile Testing. To study the mechanical properties of the filaments, a universal testing machine, Shimadzu Autograph AG-X (Kyoto, Japan) equipped with a 100 N load cell was used. The test was conducted at room temperature at a constant speed of 2 mm/min and a gauge length of 20 mm. To avoid fiber slippage, the samples were mounted on paper frames before being tested. Five replicates for each sample were tested and all samples were placed in a desiccator at 23 °C and 46% RH at least for 48 h prior to testing. The cross-section of the filaments was assumed to be circular and the diameter of the fracture point for each test sample was measured by a micrometer. The average values and standard deviations of the Young's modulus, tensile strength and strain are reported. Moreover, statistical analysis at a 5% significance level was used to test for significant difference based on the ANOVA and Tukey-HSD multiple comparison tests. In this comparison, the values for each concentration were compared with one another in the same concentration.

3. RESULTS AND DISCUSSION

3.1. Characteristics of Cellulose Nanofibers. Figure 2a shows the structure and size of the ground CNF using AFM.

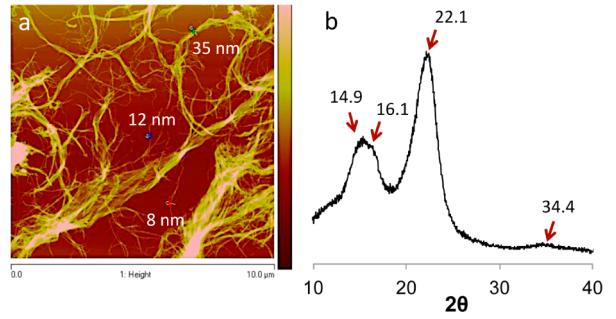

Figure 2. (a) AFM image, and (b) XRD diffractograms of the used CNF.

On the basis of the AFM study, the diameters of the finest fibers varied between 8 to 35 nm. To avoid a broadening effect, the CNF diameters were measured from height images. In addition to the isolated fibers in Figure 2a, bundles of nanofibers can be seen, which can possibly be formed during drying in sample preparation.

The XRD diffractogram of the used CNF is shown in Figure 2b. It confirms the crystallinity pattern of the native cellulose.[24,26] There are two main peaks at 14.9 and 22.1 (corresponding to lattice planes $1\bar{1}0$ and 200, respectively) and two short and broad shoulders around 16.1 and 34.4 (lattice plane 110 and 004, respectively), assigned to the diffraction of cellulose I. The crystallinity index of the CNF was calculated to 63%, based on the Segal's method, which gives a relative measure of the crystallinity.

3.2. Dry Spinning of Cellulose Filaments. Filaments were successfully prepared by dry spinning a concentrated aqueous suspension of CNF. The spinning process renders some challenges because of the air gap between collecting glass sheets and the die (20−30 cm) and also due to the low wet strength of the suspension used. In this study, a certain minimum concentration of cellulose nanofibers was required to be able to spin filaments. Concentrations from 12 down to 5 wt % were tested. In addition the manual collecting systems imposed some limitations on increasing the spinning rate.

3.3. Structure and Morphology of the Spun Filaments. The diameter of the filaments varied between 180 and 240 μm. Figure 3a shows a schematic view of the die during spinning and Figure 3b shows the visual appearance and flexibility of the filaments after drying.

Figure 4 shows the cross-sections of spun filaments with 8 and 12% CNF suspension in both 72 and 216 mm/s spinning rates. The insert figures show the surfaces of these filaments. It can be seen that the filaments are approximately circular with the exception of some flattening on one side and that there is some porosity in the filaments. The porosity is believed to be caused by air trapped in the suspension during the feeding process. However, less porosity was observed in filaments with low concentrations and high spinning speed. In addition in filaments from low concentrations a flange was formed. This is due to the contact of the wet filaments with the glass sheets. However, it is assumed that this thin structure does not affect the mechanical behavior.

DOI: 10.1021/acsami.5b03091
ACS Appl. Mater. Interfaces 2015, 7, 13022−13028

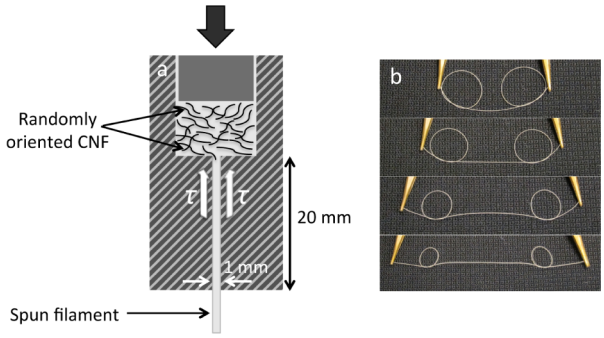

Figure 3. (a) Schematic of the die and (b) visual appearance and flexibility of the filaments.

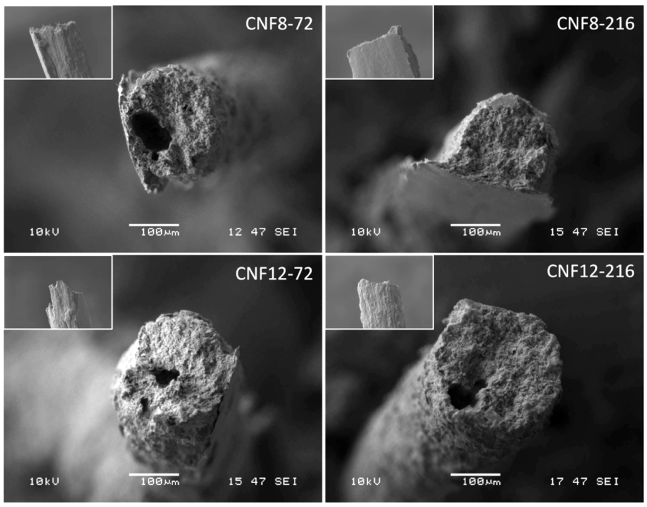

Figure 4. SEM microstructure of the filaments with 8 and 12% concentrations spun at 72 and 216 mm/s.

Figure 5 shows a high-resolution image of the surface structure of the spun filaments from the 8% concentration

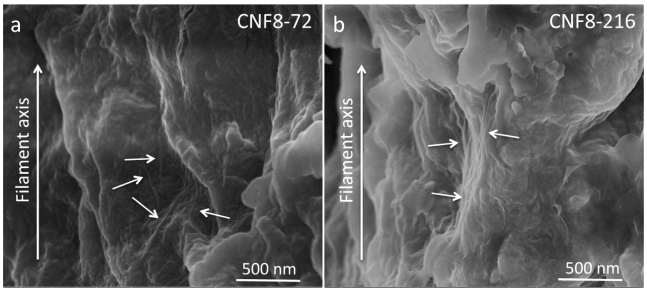

Figure 5. Surface structure of the CNF8 filaments spun with different rates of (a) 72 and (b) 216 mm/s.

suspension. It can be seen that the filament surfaces are rough and also there is evidence of partial alignment of CNF in the direction of the filament axis on the surface at both spinning rates (72 and 216 mm/s).

3.4. Orientation and Mechanical Properties of Filaments. The orientation index (f_c) and mechanical properties of all filaments were summarized in Table 2. It can be seen that there is a slight increase in the orientation as the spinning rate increases at all concentrations. A similar trend was reported by Iwamoto et al.[10] In addition, it is seen that the mechanical properties of the spun filaments are better compared to the properties of the CNF nanopaper. The properties are also slightly increased with increased spinning rate for most of the filaments being highest for the low concentrations of CNFs.

For example, for the CNF8 filaments, the strength increased from 147 to 198 MPa and the modulus from 8.3 to 11.2 GPa when the spinning rate was increased from 72 to 216 mm/s. In the case of CNF10, the increased spinning rate resulted in a significant improvement only between the lowest and highest rate. The filaments of CNF12 did not follow this trend. Increasing the spinning rate to 216 mm/s in this case decreased the strength and modulus. It is possible that it is because of porosity or inhomogeneity of the material; however, the low standard deviation does not support this. Summarizing the orientation study and mechanical properties, it is believed that increasing the spinning rate will provide a higher shear force and subsequently increase the alignment of the CNF in the filament axis direction. In general, the effect of CNF alignment on the mechanical properties is only seen in the filaments spun from low concentration suspension, thus resulting in a more organized and compact structure.

Therefore, the hypothesis that low concentration and high spinning rate would further improve the mechanical properties was tested. First, the suspension concentration was decreased to the lowest spinnable concentration (6.5 wt %) and then a maximum spinning rate was used (288 mm/s), this spinning rate being limited by the manual collection process. In addition, the spun filaments were dried under a weak tension. This new filament was coded as CNF6.5-288. Figure 6 shows the micrograph of its cross-section and surface. It can be seen that flattening still occurs, but no porosity was seen and the surface showed an orientated structure in the filament axis direction.

Figure 7 shows the XRD results and representative stress–strain curves where CNF-nanopaper, the earlier filament with the best properties (CNF8-216) and this new filament (CNF6.5-288) are compared. It can be seen that the diffractogram of the nanopaper shows a ring pattern, indicating random orientation, while the diagrams for both filaments indicate equatorial arcs corresponding to $(1\bar{1}0)$ and (200) confirming the partially orientation of the CNF. Probably the corresponding arc to (110) is merged with $(1\bar{1}0)$ on the diffractograms because of their very close scattering angles. The orientation index of the new filament was calculated to be 0.67. It is clearly seen in representative stress–strain curves that the spun filaments have better mechanical properties when compared to randomly orientated CNF-nanopaper. It is also seen that CNF6.5-288 has better mechanical properties than CNF8-216.

Figure 8 shows a 3D plot of the modulus and the strength based on the spinning rate and CNF concentration for the all spun filaments. It is seen that the modulus and strength of the latest filament (CNF6.5-288) has increased compared to the others, being 12.6 ± 1.5 GPa and 222 ± 16 MPa for modulus and strength, respectively, and its diameter decreased to 154 ± 5 μm. The modulus of CNF6.5–288 improved by 157% and the strength by 78% compared to the nanopaper. Although the mechanical properties have improved here, we believe that this partial alignment mostly happens on the filaments surface because higher mechanical properties are expected if the nanofibers are aligned throughout the filament as Sehaqui et al.[27] reported improvements of 220% for modulus and 114% for strength of the drawn cellulose nanopaper with the draw ratio of 1.6. Moreover, in another study done by Gindl-

DOI: 10.1021/acsami.5b03091
ACS Appl. Mater. Interfaces 2015, 7, 13022–13028

Table 2. Orientation Index, Fiber Diameter, Modulus, Strength and Strain at Break of All Produced Samples[a]

sample	orientation index (f_c)	diameter (μm)	modulus (GPa)	strength (MPa)	strain (%)
CNF-nanopaper			4.9 ± 0.8	125 ± 7	4.9 ± 0.9
CNF8-72	0.62	207 ± 6	8.3^{a} ± 0.8	147^{a} ± 15	3.6^{a} ± 0.3
CNF8-144	0.65	217 ± 9	7.7^{a} ± 0.6	138^{a} ± 12	3.4^{a} ± 0.5
CNF8-216	0.65	180 ± 7	11.2^{b} ± 0.9	198^{b} ± 11	3.6^{a} ± 0.6
CNF10-72	0.62	242 ± 13	7.3^{A} ± 0.5	119^{A} ± 7	2.6^{A} ± 0.7
CNF10-144	0.65	232 ± 7	$7.9^{A, C}$ ± 0.5	139^{B} ± 8	3.1^{A} ± 0.3
CNF10-216	0.68	238 ± 12	$8.4^{B, C}$ ± 0.8	145^{B} ± 17	3.1^{A} ± 0.7
CNF12-72	0.66	222 ± 10	7.8^{α} ± 0.7	131^{α} ± 15	2.8^{α} ± 0.6
CNF12-144	0.68	205 ± 9	9.1^{β} ± 0.7	152^{β} ± 15	2.7^{α} ± 0.2
CNF12-216	0.66	226 ± 8	7.7^{α} ± 0.5	$148^{\alpha, \beta}$ ± 7	4.3^{β} ± 1.3

[a]Average values with same superscript letter in the same column are not significantly different at 5% significant level based on ANOVA and Tukey-HSD comparison test. In this comparison, the values for each concentration were compared with one another in the same concentration but spun with different rates.

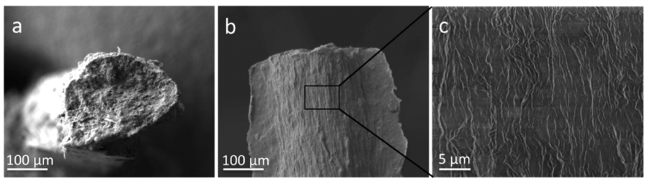

Figure 6. Microscopy image of the CNF6.5-288 filament (a) cross-section, (b) overview of the surface, and (c) detailed view showing surface orientation.

Altmutter,[28] improvements of ~370% and ~85% for modulus and strength have been reported respectively for cellulose nanopaper stretched by ratio of 1.3.

The results presented in this study are better than values reported by Torres-Rendon et al.[18] for undrawn TEMPO-oxidated CNF fibers (modulus of 8.2 ± 2.4 GPa and strength of 118 ± 12) spun with two times higher spinning rate. Though the results are slightly lower than values reported by Iwamoto et al.[10] for wood and tunicate TEMPO-oxidated CNF filaments, spun at a similar spinning rate (modulus of 19.1 ± 2.6 GPa and strength of 332 ± 93 MP for wood and modulus of 16.7 ± 2.1 GPa and strength of 282 ± 67 MPa for tunicate). However, the filaments produced here are more uniform in cross-section and can be prepared more economically and in a way that is more environmentally friendly because no chemical treatments have been used.

The theoretical modulus of the filaments can be estimated based on a rule of mixture-based micromechanical model usually implemented for short-fiber composites.[29] In a composite, the modulus, E, in the loading direction can be predicted based on the properties of the reinforcing elements and the matrix as

$$E = \eta_f \eta_o E_f \mathcal{V}_f + (1 - \mathcal{V}_f) E_m \tag{3}$$

where

$$\eta_f = 1 - \frac{\tanh(\beta l/2)}{\beta l/2} \tag{4}$$

and

$$\beta = \frac{1}{r_f}\sqrt{\frac{2G_m}{E_f \ln(R/r_f)}} \tag{5}$$

where E_f is the elastic modulus of the CNF, V_f is the CNF volume fraction and was determined from the measured density of the CNF6.5-288 filament (1.37 g/cm^3) and density of cellulose I$_\beta$ (1.64 g/cm^3).[30] η_f is the CNF length efficiency given by eq 4 and η_o is an orientation factor which is assumed to be 1 to show the potential of the fully aligned CNF on the modulus of the filament. The $(1 - V_f)E_m$ term is zero and the shear modulus, G_m, is the bond shear modulus between the CNF since in this case there is no matrix. G_m was taken from back-calculations that have been done in earlier work based on CNF networks.[31] l is the length of the CNF and was assumed as 1 μm, r_f is the fiber radius and set to the average value obtained from AFM image measurement, R/r_f is the ratio of the interfiber distance to the CNF radius, which can be calculated from $(K_R/V_f)^{1/2}$, where K_R is a packing number, which for parallel hexagonal packing is 0.907,[32] and is the number used

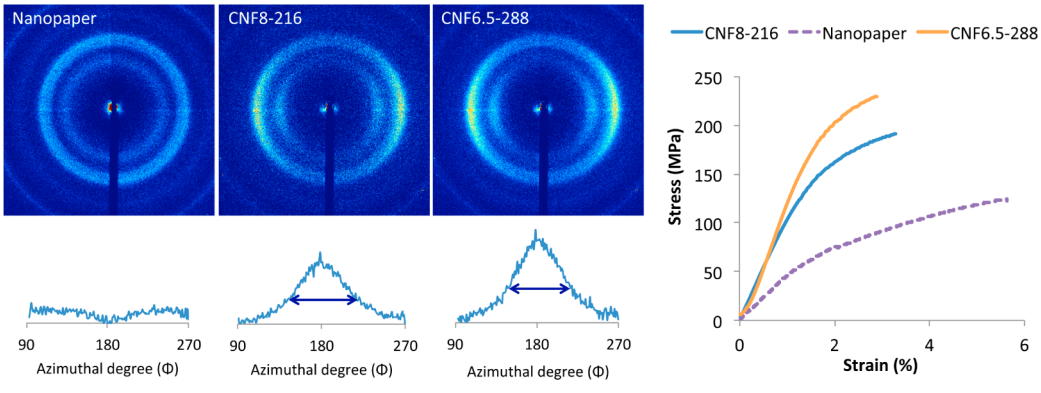

Figure 7. X-ray diffractograms and representative stress–strain curves of the prepared CNF-nanopaper, CNF8-216, and CNF6.5-288.

DOI: 10.1021/acsami.5b03091
ACS Appl. Mater. Interfaces 2015, 7, 13022–13028

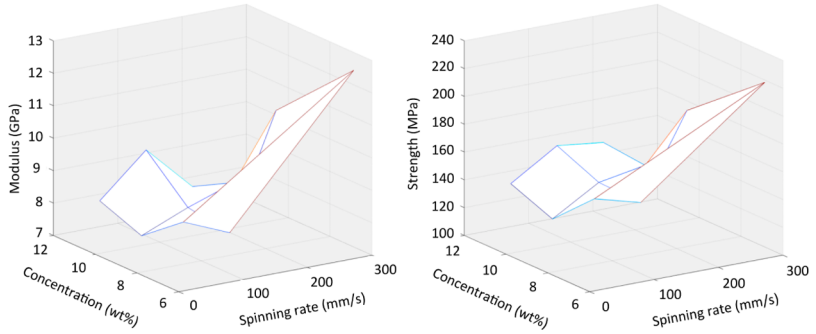

Figure 8. 3D plots of the modulus and strength of the produced filaments where the effect of spinning rate and CNF concentration are taken into account.

here for this highly packed filament. The parameter values used in this model as well as the theoretical stiffness of the filament are summarized in Table 3.

Table 3. Parameters Used in the Short Fiber Model, Described by Eqs 3−5, To Calculate the Theoretical Value of the Modulus of the CNF6.5-288 in the Case of 100% CNF Alignment in the Filament

parameter	value
E_f (GPa)	135[33]
E_m (GPa)	0
G_m (MPa)	100
V_f (%)	83
R/r_f	1.04
r_f (nm)	9.15
l (nm)	1000
β (x1e^6)	19.75[a]
η_o	1
η_f	0.9[a]
E (GPa)	101[a]

[a]Calculated values from eqs 3−5.

From eq 1, the theoretical modulus is 101 GPa assuming all the CNF are orientated. With the CNF6.5-288 filament giving a stiffness of 12.6 GPa, this indicates that the orientation must be very low or just on the surface of the filaments. It is also possible that the CNFs used here have a lower modulus that the estimated 135 GPa.

4. CONCLUSIONS

Dry spinning of cellulose nanofibers (CNF) based on banana waste were successfully made using piston-driven extrusion (capillary rheometer). The effect of CNF concentration in the suspensions as well as the spinning rate was evaluated. The results are very promising. The filaments showed good mechanical properties, which were increased with increased spinning rate and decreased CNF concentration. X-ray confirmed that the orientation index of CNF in the filaments was increased with increased spinning rate. Fracture surface study of the filaments showed that the filaments spun with low CNF concentration had a denser structure.

Although the mechanical properties did not reach the level of natural fibers such as soft wood fibers (40 GPa), even at this initial stage, the properties are similar to regenerated cellulose filaments (viscose 11 GPa) and the fact that these filaments are based on native cellulose and produced from biomass waste using a simple spinning process without any additional chemicals, mean they have considerably potential for further development. The filaments produced here are relatively uniform in cross-section and can be prepared economically and in an environmental friendly way with no chemical treatments.

Thus, we believe that by using suitable nanofiber concentrations together with an improved processing procedure, even higher mechanical properties can be achieved.

AUTHOR INFORMATION

Corresponding Author

*E-mail: kristiina.oksman@ltu.se. Phone: +46 920 493371.

Notes

The authors declare no competing financial interest.

ACKNOWLEDGMENTS

The authors gratefully acknowledge the Bio4Energy for the financial support of this work, the ECLIPSE project for supplied bleached banana rachis fibers (grant agreement 280786), Zoheb Karim and Natalia Herrera for CNF fibrillation, Dr. Iftekhar Uddin Bhuiyan and Johnny Grahn for help with XHR-SEM and SEM studies, and Dr. Danil Korelskiy and Natalia Dadivanyan for XRD and 2D-WAXRD examinations.

REFERENCES

(1) Zadorecki, P.; Michell, A. J. Future Prospects for Wood Cellulose as Reinforcement in Organic Polymer Composites. *Polym. Compos.* **1989**, *10*, 69−77.

(2) Bledzki, A. K.; Gassan, J. Composites Reinforced with Cellulose Based Fibres. *Prog. Polym. Sci.* **1999**, *24*, 221−274.

(3) Wambua, P.; Ivens, J.; Verpoest, I. Natural Fibres: Can They Replace Glass in Fibre Reinforced Plastics? *Compos. Sci. Technol.* **2003**, *63*, 1259−1264.

(4) Chabba, S.; Matthews, G. F.; Netravali, A. N. 'Green' Composites Using Cross-Linked Soy Flour and Flax Yarns. *Green Chem.* **2005**, *7*, 576−581.

(5) Chabba, S.; Netravali, A. 'Green' Composites Part 2: Characterization of Flax Yarn and Glutaraldehyde/Poly(Vinyl Alcohol) Modified Soy Protein Concentrate Composites. *J. Mater. Sci.* **2005**, *40*, 6275−6282.

(6) Goutianos, S.; Peijs, T.; Nystrom, B.; Skrifvars, M. Development of Flax Fibre Based Textile Reinforcements for Composite Applications. *Appl. Compos. Mater.* **2006**, *13*, 199−215.

(7) Hooshmand, S.; Cho, S.; Skrifvars, M.; Mathew, A. P.; Oksman, K. Melt Spun Cellulose Nanocomposite Fibres: Comparison of Two Dispersion Techniques. *Plastic Rubber Compos.* **2014**, *43*, 15−24.

(8) Hooshmand, S.; Aitomäki, Y.; Skrifvars, M.; Mathew, A.; Oksman, K. All-Cellulose Nanocomposite Fibers Produced by Melt

DOI: 10.1021/acsami.5b03091
ACS Appl. Mater. Interfaces 2015, 7, 13022−13028

Spinning Cellulose Acetate Butyrate and Cellulose Nanocrystals. *Cellulose* **2014**, *21*, 2665−2678.
(9) Johnson, R. K.; Zink-Sharp, A.; Renneckar, S. H.; Glasser, W. G. Mechanical Properties of Wetlaid Lyocell and Hybrid Fiber-reinforced Composites with Polypropylene. *Composites, Part A* **2008**, *39*, 470−477.
(10) Iwamoto, S.; Isogai, A.; Iwata, T. Structure and Mechanical Properties of Wet-Spun Fibers Made from Natural Cellulose Nanofibers. *Biomacromolecules* **2011**, *12*, 831−836.
(11) Nishino, T.; Takano, K.; Nakamae, K. Elastic Modulus of the Crystalline Regions of Cellulose Polymorphs. *J. Polym. Sci., Part B: Polym. Phys.* **1995**, *33*, 1647−1651.
(12) Zeronian, S. H. Mechanical Properties of Cotton Fibers. *J. Appl. Polym. Sci.: Appl.* **1991**, *47*, 445−461.
(13) Chen, P.; Kim, H.; Kwon, S.; Yun, Y. S.; Jin, H. Regenerated Bacterial Cellulose/Multi-walled Carbon Nanotubes Composite Fibers Prepared by Wet-Spinning. *Curr. Appl. Phys.* **2009**, *9*, 96−99.
(14) Herrick, F. W.; Casebier, R. L.; Hamilton, J. K.; Sandberg, K. R. Microfibrillated Cellulose: Morphology and Accessibility. *J. Appl. Polym. Sci.* **1983**, *37*, 797−813.
(15) Turbak, A. F.; Snyder, F. W.; Sandberg, K. R. Microfibrillated Cellulose, a New Cellulose Product: Properties, Uses, and Commercial Potential. *J. Appl. Polym. Sci.* **1983**, *37*, 815−827.
(16) Van den Berg, O.; Schroeter, M.; Capadona, J. R.; Weder, C. Nanocomposites Based on Cellulose Whiskers and (Semi)Conducting Conjugated Polymers. *J. Mater. Chem.* **2007**, *17*, 2746−2753.
(17) Walther, A.; Timonen, J. V. I; DÃez, I.; Laukkanen, A.; Ikkala, O. Multifunctional High-Performance Biofibers Based on Wet-Extrusion of Renewable Native Cellulose Nanofibrils. *Adv. Mater.* **2011**, *23*, 2924−2928.
(18) Torres-Rendon, J. G.; Schacher, F. H.; Ifuku, S.; Walther, A. Mechanical Performance of Macrofibers of Cellulose and Chitin Nanofibrils Aligned by Wet-Stretching: A Critical Comparison. *Biomacromolecules* **2014**, *15*, 2709−2717.
(19) Håkansson, K. M. O.; Fall, A. B.; Lundell, F.; Yu, S.; Krywka, C.; Roth, S. V.; Santoro, G.; Kvick, M.; Prahl Wittberg, L.; Wågberg, L.; Söderberg, L. D. Hydrodynamic Alignment and Assembly of Nanofibrils Resulting in Strong Cellulose Filaments. *Nature Commun.* **2014**, *5*, 1−10.
(20) Jiang, C.; Saha, A.; Young, C. C.; Hashim, D. P.; Ramirez, C. E.; Ajayan, P. M.; Pasquali, M.; Martí, A. A. Macroscopic Nanotube Fibers Spun from Single-Walled Carbon Nanotube Polyelectrolytes. *ACS Nano* **2014**, *8*, 9107−9112.
(21) Mohapatra, D.; Mishra, S.; Sutar, N. Banana and Its By-Product Utilization: An Overview. *J. Sci. Ind. Res.* **2010**, *69*, 323−329.
(22) FAO (Food and Agricultural Organization of the United Nations). www.fao.org.
(23) Persson, M.; Lorite, G. S.; Cho, S.; Tuukkanen, J.; Skrifvars, M. Melt Spinning of Poly(Lactic Acid) and Hydroxyapatite Composite Fibers: Influence of the Filler Content on the Fiber Properties. *ACS Appl. Mater. Interfaces* **2013**, *5*, 6864−6872.
(24) Segal, L.; Creely, J.; Martin, A.; Conrad, C. An Empirical Method for Estimating the Degree of Crystallinity of Native Cellulose Using the X-ray Diffractometer. *Text. Res. J.* **1959**, *29*, 786−794.
(25) Tanaka, T.; Fujita, M.; Takeuchi, A.; Suzuki, Y.; Uesugi, K.; Ito, K.; Fujisawa, T.; Doi, Y.; Iwata, T. Formation of Highly Ordered Structure in Poly[(R)-3-Hydroxybutyrate-Co-(R)-3-Hydroxyvalerate] High-Strength Fibers. *Macromolecules* **2006**, *39*, 2940−2946.
(26) Segal, L.; Conrad, C. Characterization of Cellulose Derivatives by Means of the X-ray Diffractometer. *Am. Dyest. Rep.* **1957**, *46*, 637−642.
(27) Sehaqui, H.; Ezekiel Mushi, N.; Morimune, S.; Salajkova, M.; Nishino, T.; Berglund, L. A. Cellulose Nanofiber Orientation in Nanopaper and Nanocomposites by Cold Drawing. *ACS Appl. Mater. Interfaces* **2012**, *4*, 1043−1049.
(28) Gindl-Altmutter, W.; Veigel, S.; Obersriebnig, M.; Tippelreither, C.; Keckes, J. In *Functional Materials from Renewable Sources*; Falk, L., Thomas, R., Eds.; American Chemical Society: Washington, D.C., 2012; Chapter 1, pp 3−16.
(29) Andersons, J.; Sparnins, E.; Joffe, R. Stiffness and Strength of Flax Fiber/Polymer Matrix Composites. *Polym. Compos.* **2006**, *27*, 221−229.
(30) Ganster,J.; Fink, H. In *Polymer Handbook*, 4th ed; Brandrup, J., Immergut, E. H. Grulke, E. A., Eds.; Wiley−Interscience: New York, 1998; Vol *1*, Chapter 5, pp 136.
(31) Aitomäki, Y.; Oksman, K. Reinforcing Efficiency of Nanocellulose in Polymers. *React. Funct. Polym.* **2014**, *85*, 151−156.
(32) Landel, R. F.; Nielsen, L. E. In *Mechanical Properties of Polymers and Composites*, 2nd ed; Marcel Dekker: New York, 1974; Chapter 7, pp 380.
(33) Sakurada, I.; Nukushina, Y.; Ito, T. Experimental Determination of the Elastic Modulus of Crystalline Regions in Oriented Polymers. *J. Polym. Sci.* **1962**, *57*, 651−660.

DOI: 10.1021/acsami.5b03091
ACS Appl. Mater. Interfaces 2015, 7, 13022−13028